Journal of
Composites Science

MDPI

Article

Water Diffusion in Additively Manufactured Polymers: Effect of Voids

Boyu Li, Konstantinos P. Baxevanakis and Vadim V. Silberschmidt *

Wolfson School of Mechanical, Electrical and Manufacturing Engineering, Loughborough University, Loughborough LE11 3TU, UK; b.li4@lboro.ac.uk (B.L.); k.baxevanakis@lboro.ac.uk (K.P.B.)
* Correspondence: v.silberschmidt@lboro.ac.uk; Tel.: +44-(0)15-0922-7504

Abstract: This study investigates the effect of void features in additively manufactured polymers on water diffusion, focusing on polyethylene terephthalate glycol (PETG) composites. The additive manufacturing (AM) of polymers, specifically, material extrusion AM (MEAM), results in manufacturing-induced voids, therefore affecting the water resistance of the printed parts. The research analyses the effects of size, shape, orientation and the hydrophilicity of voids on moisture diffusion in PETG composites employing numerical (finite-element) simulations. Two void types were examined: voids of Type I that retard the moisture propagation and voids of Type II that enhance it. Simulations demonstrate that a higher volume fraction of voids and their orientation with regard to the diffusion direction significantly hinder the moisture transport for Type I voids. Conversely, due to their high diffusivity, Type II voids serve as channels for rapid moisture transmission. Consequently, for such materials, the global diffusion rates mainly depend on the volume fraction of voids rather than their shape. These findings indicate the critical role of voids in the design of AM parts for environments exposed to moisture, such as marine and offshore applications. Understanding the void effects is critical for optimising the durability and performance of MEAM components underwater exposure.

Keywords: additive manufacturing; composite material; water diffusion; void; finite-element modelling

Citation: Li, B.; Baxevanakis, K.P.; Silberschmidt, V.V. Water Diffusion in Additively Manufactured Polymers: Effect of Voids. *J. Compos. Sci.* **2024**, *8*, 319. https://doi.org/10.3390/jcs8080319

Academic Editor: Francesco Tornabene

Received: 28 June 2024
Revised: 25 July 2024
Accepted: 8 August 2024
Published: 12 August 2024

1. Introduction

Additive manufacturing (AM) is a widely used method with potential applications in various sectors, including the shipbuilding and biomedical industries [1–4]. Alongside metallic materials, AM widely uses polymers, employing Fused Deposition Modelling based on mechanical extrusion, also known as *material extrusion additive manufacturing* (MEAM). Among polymers, polyethylene terephthalate glycol (PETG) is one of the mainstream materials in AM as it demonstrates excellent mechanical properties and chemical resistance. Thanks to these properties, it has a significant potential in naval structures and for other uses in the marine environment [5]. However, the degradation of 3D-printed PETG as a result of its exposure to water is one of the major challenges that should be considered during the design and manufacture of components for the maritime sector.

Li et al. [6] explored the hygrothermal degradation of traditional carbon fibre (CF) woven/PETG sheet-laminated composite (produced using hot-press moulding) at 20 °C, 45 °C and 60 °C for 90 days. PETG specimens reinforced with CF-woven fabric absorbed less water than pure PETG samples at all the studied test temperatures. The flexural strength of such specimens exhibited a decrease ranging from 28.6% to 32.2% across a temperature range of 25 °C to 60 °C. PETG specimens produced with material extrusion AM (MEAM) after immersing in salt water at 30 °C for 21 days demonstrated a reduction in tensile strength of 6.36%, as was found in [7]. Compared to polylactic acid (PLA) and polycarbonate (PC), PETG specimens showed a better resistance to water ageing. The

extent of reduction in mechanical performance after water ageing is one of the critical factors for many naval applications.

Microstructural analysis with scanning electron microscopy (SEM) of specimens failed in a 3-point bending test, which showed that the absorbed water mainly influenced the interface area, leading to debonding between the matrix and fibres. For MEAM composite materials, the gaps between layers, voids and other defects generated during their manufacture led to higher levels of water diffusivity and absorption rate as well as a larger surface area for water permeation [8]. Also, surface roughness affects diffusivity by varying the surface area; it is linked to layer thickness, printing speed, nozzle temperature and other manufacturing factors [9].

Current research on water diffusion in composite material focuses on Fick's or Langmuir's diffusion in the matrix by considering it as a homogeneous material [10]. However, various researchers indicate that manufacturing-induced voids in MEAM structures are unavoidable, significantly increasing the volume fraction of porosity in the printed samples [11,12]. The dimensions and shape of voids are related to the insertion of reinforcement material [13], the gap between the contour layer and the infill zone due to the printing line width [14], the infill pattern, etc. The research of Goh et al. [15] found voids with a size of more than 16.4 μm in the matrix of MEAM carbon- or glass-fibre-reinforced nylon. Voids due to the imperfect bonding between the fibre and the matrix were also observed [16].

Alongside the entrapment of air and volatile components evolving from the resin during liquid processing of the composite, the shrinkage of the matrix after curing leads to voids in the interphase area between the matrix and fibres [17]. For an AM material, voids between beads formed during 3D printing were found with a diameter of less than 30 μm or more than 100 μm [18] (Figure 1). The size of voids with triangular cross-sections between beads could be reduced by increasing the volume fraction of fibres or diminishing the layer thickness. Such voids have an additional further influence on diffusion in the through-thickness, longitudinal and transverse directions.

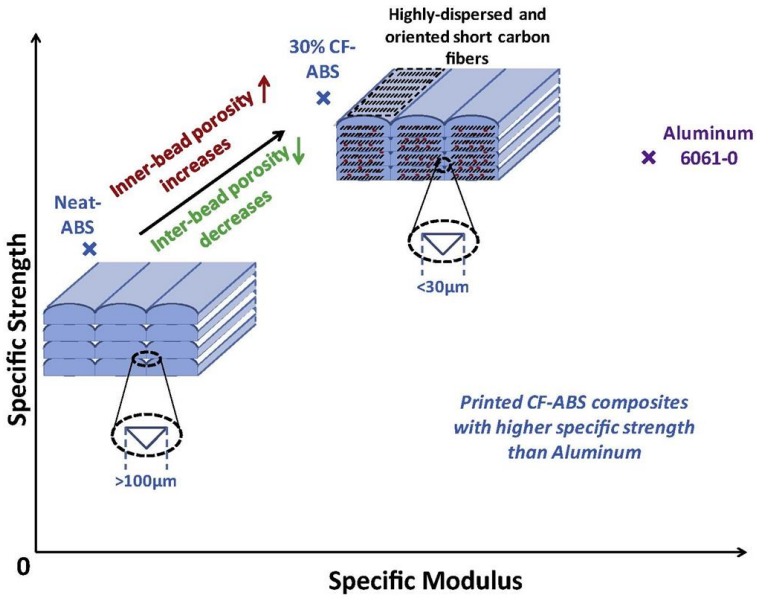

Figure 1. Schematic presentation of 3D-printed fibre-reinforced composite manufactured with MEAM [18].

Historically, research into diffusion in polymers started on materials produced with traditional (i.e., non-AM) processes. Abdelmola and Carlsson [19] examined the effect of voids on water diffusion in epoxy with different volume fractions of voids by adding different amounts of surfactant and blowing agent. The microscopic analysis indicated that the artificially generated voids were spherical, and their diameter was much less than the specimen thickness. Specimens that use both surfactant and blowing agent were influenced

by the voids most significantly and some of the voids in the matrix were connected. The water-uptake experiment demonstrated that the matrix's voids substantially accelerated the diffusion process. The content of moisture in specimens with low and medium void fractions was slightly higher than that in the pure-matrix sample. However, in specimens with a volume fraction of voids in the range from 50% to 60%, moisture absorption was significantly higher than in materials with lower porosity, likely due to water filling the connected voids. Futhermore, studies with differential scanning calorimetry (DSC) and dynamic mechanical analysis (DMA) were conducted on the specimens with different volume fractions of voids to investigate the effect on the glass transition temperature T_g before and after water ageing. No variation in T_g was found during water ageing of specimens with different microstructures.

Wang [20] explored the effects of the volume fraction of voids, their size and shape on the water diffusion in plain woven composites with finite-element (FE) analysis both at micro- and meso-scales. In the developed model, carbon fibres were assumed to be hydrophobic and the water diffusion rate in the void was ten times higher than in the matrix. The voids were randomly generated to simulate the manufacturing-induced defects in the composite material. According to the simulation results, the diffusion rate in all directions was proportional to the void volume fraction. The mass diffusion rate in the thickness direction increased as the void size expanded, whereas the in-plane diffusion rate decreased with the increasing void size. Furthermore, the standard deviation increased significantly with larger void sizes. This could be explained by the growing extent of randomness in models with a constant void volume fraction but fewer (i.e., larger) voids. To assess the effect of the shape of voids, spherical and ellipsoidal voids were considered. The former led to a lower diffusion rate, especially in cases of their higher eccentricity. Hocine et al. [21] investigated the effect of an elliptical crack-shaped cavity aligned along the x-axis of a matrix on water diffusion. The void significantly accelerated the diffusion process when moisture penetrated in the x direction. This was because water vapour in the cavity had higher diffusivity compared to that for the matrix. Conversely, the void had a minor contribution when the diffusion was along the y direction. The study also employed models with cavities with different aspect ratios, revealing anisotropic diffusion when the voids were flat. In contrast, a model with a round void exhibited isotropic diffusion characteristics. Additionally, the distribution effect of multiple voids was studied. For elongated elliptical cavities, their increased aspect ratio led to a greater impact on the diffusion process. Furthermore, models with numerous small voids displayed more isotropic diffusivity than those with fewer, larger voids in the case of the constant volume fraction of voids.

In AM materials, the voids are usually aligned regularly between printing beads as shown in Figure 2. Such voids are due to the shrinkage of the matrix during cooling, and their size aligns with the findings of Tekinalp et al. [18]. This allows to use of a model of a representative volume element (RVE) in FE analysis to gain a deeper understanding of water diffusion within the specimen.

To construct a detailed RVE model, it is important to obtain an accurate value of the volume fraction of voids and their dimensions. Multiple methods were applied for the analysis of voids in composites [17]. Direct measurements of material density are one of the most affordable and straightforward ways to determine the level of porosity, as voids do not contribute to the material's mass. However, the density of the pure matrix is always inaccurate due to unavoidable curing-induced voids. Additionally, for fibre-reinforced composites, assessing the volume fraction and mass of fibres by burning off the matrix or dissolving it with a chemical solvent introduces errors, as the residual matrix remains on the fibres after the treatment; also, the fibres can be damaged during the procedure. Little et al. [22] explored the properties of voids in epoxy with micro-CT scanning with a resolution of 7 μm. Voids below this resolution threshold—some 20% of the total—were undetected. Still, they constitute less than 0.5% of the total void volume, having a negligible impact on water diffusion in the composite material. Although micro-CT can accurately

describe the shape, size and location of voids, the required increase in the scan resolution increased its cost and time. In a traditional microscopic analysis, a destructive cutting is required to inspect the cross-section of the specimen. As a result, the acquired shapes and dimensions of voids are restricted to a 2D plane.

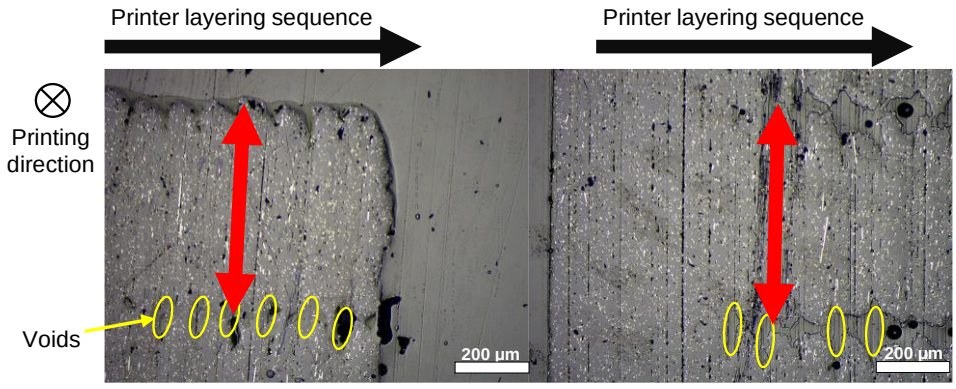

Figure 2. Transversal cross-section of 3D-printed PETG specimen reinforced with short carbon fibres.

In this study, an FE-based assessment of the effect of voids in a MEAM composite is performed at a microscale with the ABAQUS 2023 software package. The study focuses on the impact of void shape and size on water diffusion linked to the moisture transport in the matrix. At this stage of research, the contribution of fibres to the diffusion process is not considered.

2. Methodology

Microscale finite-element models for a polymer domain with different inter-bead voids are shown in Figure 1. The size of the model is 0.2 mm by 0.2 mm. Water diffusion in models with different sizes and shapes of voids shown in Figure 3 was simulated and compared to understand the diffusion around the voids further. Following a separate mesh sensitivity study, a quadratic-dominated mesh with element size of 0.001 mm was applied to the circular, diamond and pure matrix models. For the triangular-void model, 0.001 mm triangular elements were used to better fit the contours of the void. Such a finer mesh, compared to elements commonly used in models of 3D-printed composites with dimensions of around 1 mm (see, e.g., [23]), was required for microscopic simulations due to the characteristic dimensions of the defects.

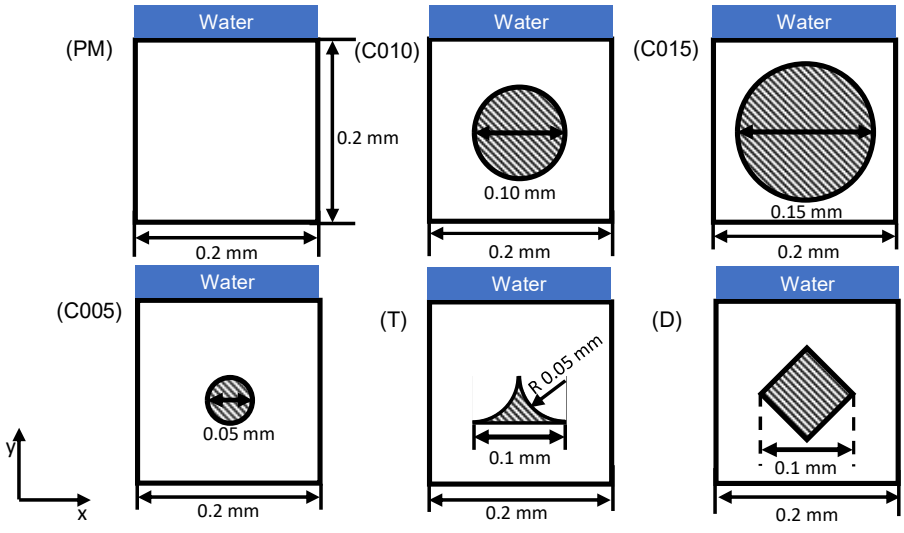

Figure 3. Schematics of 0.2 mm × 0.2 mm FEA models: (PM) no void; (C010), (C015) and (C005) circular voids; (T) triangular void; (D) diamond-shape void.

Table 1 provides notation for the implemented FE models of polymers with different voids and corresponding levels of porosity that change from 2.7% for triangular voids to 44.2% for the largest cylindrical pore. The case of pure matrix (i.e., with a porosity of 0%) was considered as a reference.

Table 1. Notation of FE models and volume fraction of voids in them.

Void Shape	Pure Matrix	Triangle and Inverted Triangle	Diamond	Circle ∅0.05 mm	Circle ∅0.10 mm	Circle ∅0.15 mm
Model notation	PM	T and IT	D	C005	C010	C015
The volume fraction of void	0%	2.7%	17.7%	4.9%	19.6%	44.2%

In the research of Wang [20], an assumption of the hydrophilic character of the modelled material was made, and, therefore, two types of voids are compared in the FE model as shown in Table 2: Voids of Type I are completely hydrophobic, while those of Type II are filled with air and absorb moisture from the water vapour in the air. Such assumptions, related to extreme cases of the material's hygroscopic response, are related to the lower and upper bonds of diffusivity. Some researchers [20,24] assumed that the diffusivity in the void was ten times larger compared to the matrix. This assumption highlights the importance of void parameters in influencing the diffusion process within the matrix.

Table 2. Water diffusion coefficient of PETG matrix and voids of different types.

Material	Ageing Temperature (°C)	Diffusivity (mm²/ms)	Maximum Water Uptake in Volume (%)
PETG *	25	8.02×10^{-4}	0.55
Void Type I	25	0	0
Void Type II	25	0.026 **	0.55

* From [6]. ** From [25].

For maximum water uptake in voids of Type II, it is assumed that the maximum amount of water absorbed is equivalent to the amount absorbed in the matrix. A further sensitivity analysis of the maximum water uptake in the void is shown in Figure 4. By reducing water solubility in a void tenfold compared to that in PETG, the saturation time was only slightly reduced. Conversely, increasing the solubility by 10 times significantly increased the saturation time. By reducing solubility to 10% of the water solubility, the saturation time is only slightly reduced. The sample saturated even slower than in the case of the pure-matrix model.

The global water concentration $\langle C \rangle$ was calculated by dividing the sum of water volumes in each matrix element by the total volume in the matrix in ABAQUS:

$$\langle C \rangle = \frac{\sum_i C_i V_i}{\sum_i V_i}$$

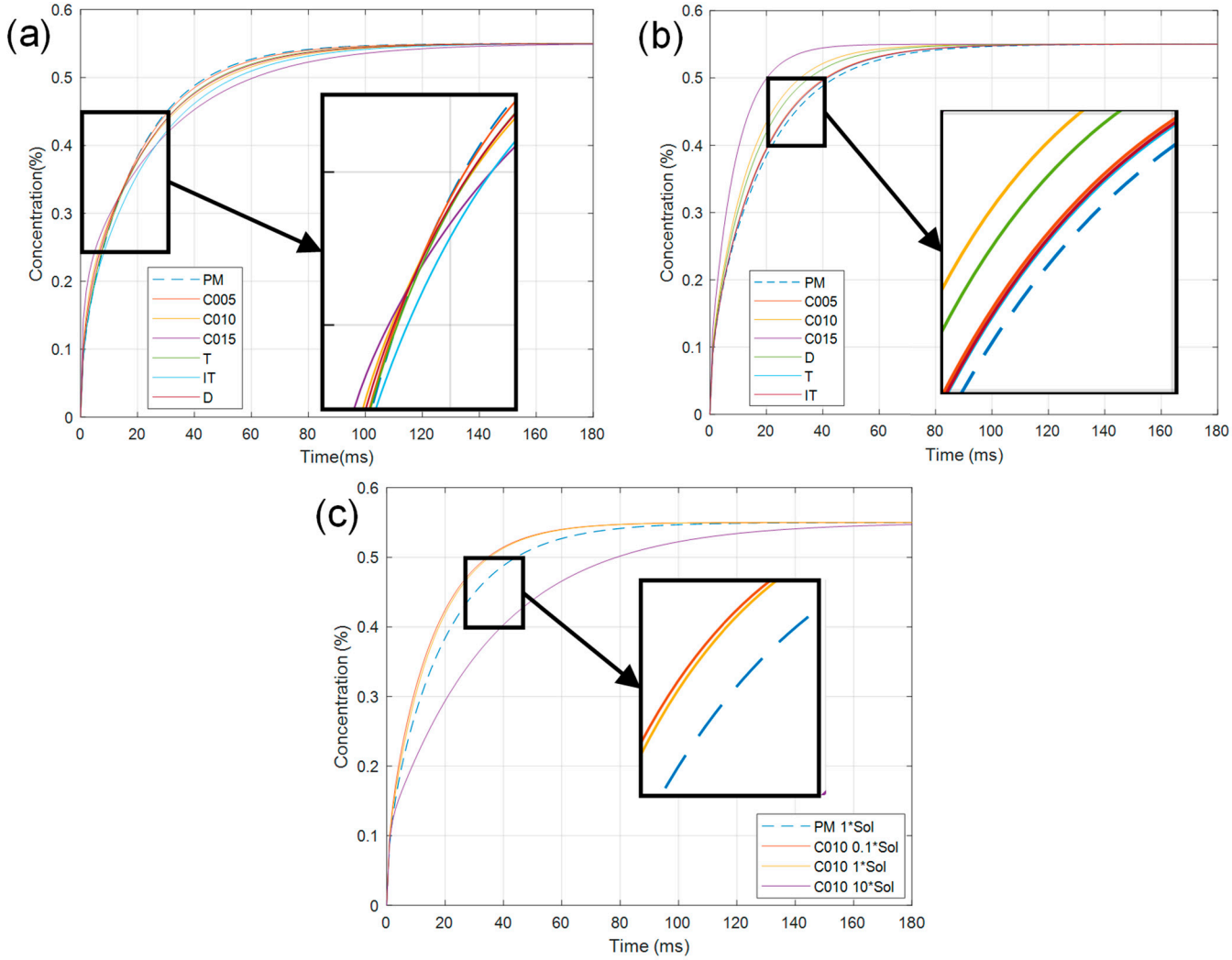

Figure 4. Evolution of water uptake for different void shapes: (**a**) Type I; (**b**) Type II. (**c**) Effect of solubility on water uptake.

3. Results and Discussion

Numerical simulations of water diffusion were implemented with ABAQUS for all the void shapes and types to elucidate its thermo-spatial evolution. The results of the analysis for Type I voids demonstrated that the inverted-triangular and the circular void with the largest diameter had the most significant retardation effect on moisture diffusion (Figure 4a). The rest of the models underwent saturation following a specific sequence of void shapes and sizes: the circular void with a diameter of 0.10 mm, followed by the diamond-shaped void, then the triangular void and, finally, the smallest circular void (with a diameter of 0.05 mm). This saturation pattern may be attributed to the volume fraction of the voids, as detailed in Table 1, with large hydrophobic voids restricting the moisture propagation into the matrix. Table 1 provides notation for the implemented FE models of polymer with different voids and corresponding levels of porosity that change from 2.7% for triangular voids to 44.2% for the largest cylindrical pore. The case of pure matrix (i.e., with porosity of 0%) was considered as a reference.

Apart from the volume fraction, the shape of the voids and their orientation about the water-penetration direction significantly impacted the diffusion process. The time to reach a 90% saturation time increased by up to one-third compared to that for the pure matrix model. For instance, the wide top side of the inverted-triangle void obstructed the water absorption. As is obvious from Figure 5, the concentration contour for 5 ms indicates that this top edge of the IT void created a barrier to moisture transport compared with the

case of the triangular void of the same dimensions. This barrier effect was primarily due to the reduction in the cross-sectional area available for diffusion, effectively restricting the moisture propagation through the matrix.

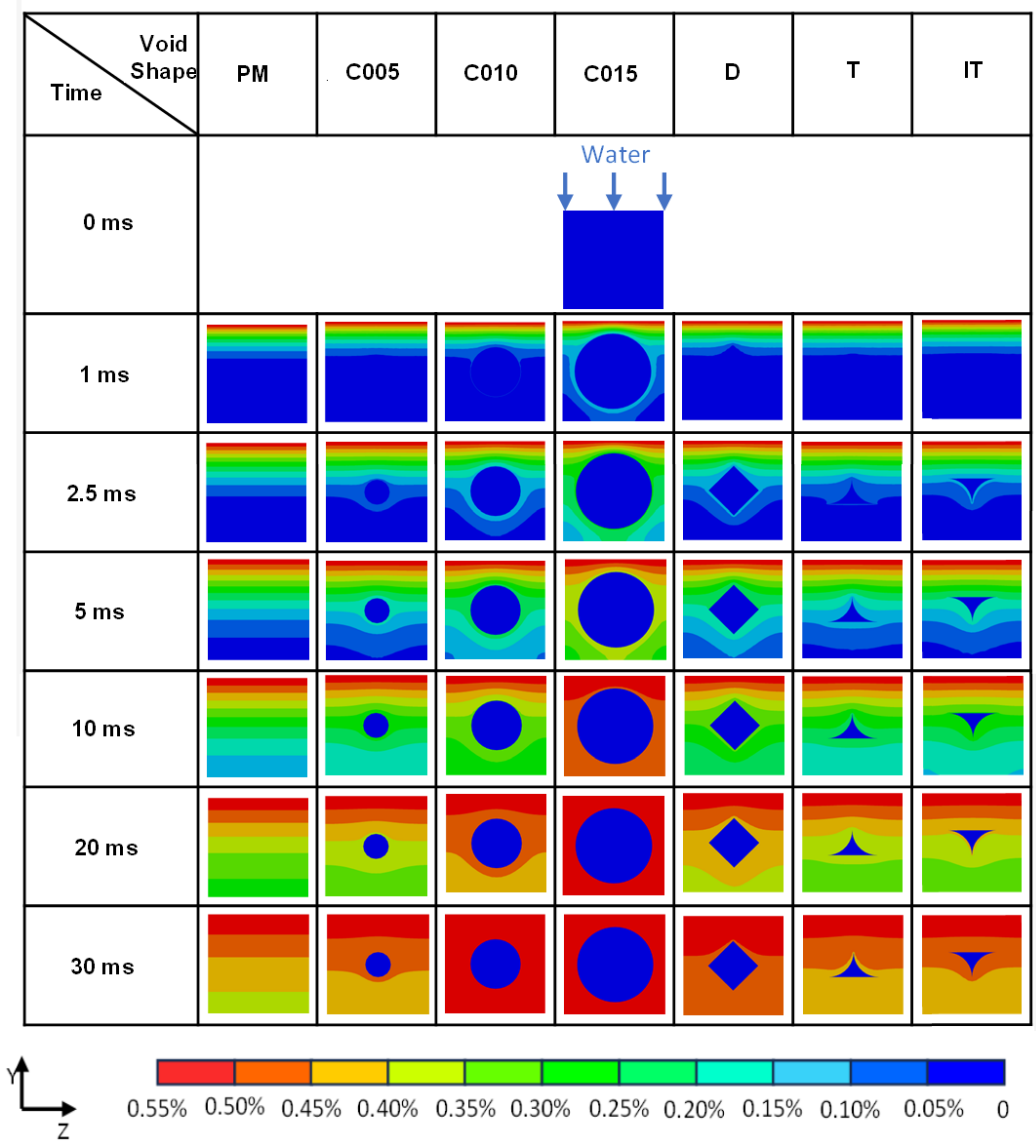

Figure 5. Spatial evolution of water uptake process for different voids of Type I.

In contrast to the T and IT models, with their voids positioned away from the top edge of the analysed domain, other void configurations exhibited higher initial moisture concentrations when compared to the pure matrix. The central region of the top layer reached the saturation state earlier than the peripheral elements (Figure 5). This early saturation phenomenon was caused by the voids' hydrophobic character, which prevented water penetration, accumulating moisture in the adjacent elements. After 10–20 ms of the diffusion process, the concentration curves of the rest of the models intersected with that of the pure matrix.

The simulated development of the mass flow rate (see Figure 6) provided further insight into the moisture transport path and the distribution of fluid in the models. The central region in the area adjacent to the water-exposed top edge had a higher mass flow rate compared to the elements in the peripheral horizontal parts. The opposite situation was observed at the bottom part of the model: the central region showed a substantially lower mass flow rate compared to the peripheral elements since the water propagated from

the horizontal peripheral elements. This observation confirmed that moisture movement was influenced by the hydrophobic void edges. For the C015 model, the time to reach 0.5% concentration of moisture was 20% more than for the pure-matrix model.

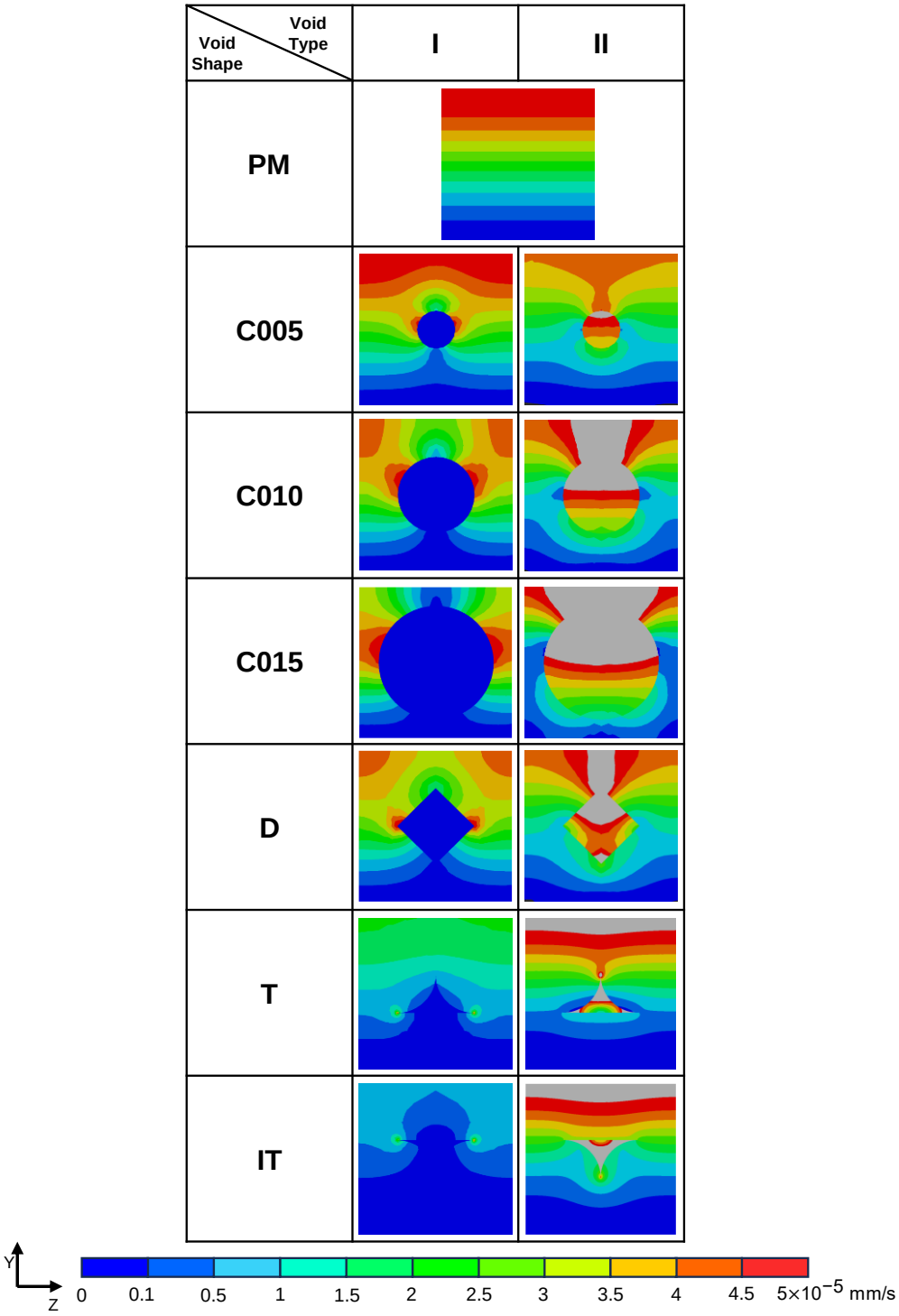

Figure 6. Mass flow rate at 5 ms calculated with FEM models.

Therefore, in a situation of a hydrophobic void, its shape has a notable influence on the direction and amount of flow in the local area. Such voids could also create barriers to moisture diffusion by limiting the channel size.

The models of Type II demonstrated a different behaviour (Figure 4b). Here, the model containing a circular void with a diameter of 0.15 mm reached saturation first. It

was followed by the models in the following order: C010, D, C005, IT and, finally, T. The obtained results demonstrated that the hydrophilic (Type II) voids could significantly affect the transport of moisture and the overall diffusivity of the porous materials. The sequence, in which the models reached the saturation state, corresponded to the volume fraction of voids (Table 1): the higher the level of porosity, the earlier the transition to saturation. Comparing the T and C005 models, the triangular void has a longer perimeter (i.e., surface contacting with the water) compared to the circular one, despite the former having a smaller void volume fraction. Consequently, the triangular models could transmit the moisture more effectively. This result indicates that when the voids can effectively transport moisture and have significantly higher diffusivity than the matrix, the overall diffusivity of the material depends on the volume fraction of the void. Furthermore, the geometric shape of the voids also contributes to the level of effective diffusivity. Voids with larger perimeters exhibited higher diffusion efficiency than circular voids with a similar volume fraction. However, this could not explain the difference in diffusion efficiency between the T and IT models. A further explanation based on the mass flow rate diagram is given below.

The spatial evolution of the diffusion process across various models at different time intervals is presented in Figure 7 for Type II voids. Initially, within the first millisecond, there was no significant difference in moisture penetration between most models and the reference-pure-matrix model. This was because only a minimal amount of moisture entered the voids during this brief period. However, C015 demonstrated some deviation from this development: a thin layer of elements surrounding the bottom of the void displayed a higher moisture concentration compared to the adjacent matrix. This was a consequence of the large hydrophilic void, transmitting moisture to the surrounding elements more effectively than the matrix. By 2.5 ms, the voids in most models transferred the moisture to the surrounding elements and accelerated the diffusion process. However, in the T model, the diffusion was less pronounced than in other models due to the limited interface area facing the flow direction, which restricted the moisture transfer. This variation in diffusion effectiveness is consistent with the findings presented in Figure 3: the concentration curves have large upward deviations from that for the pure matrix after the initial stage. At 5 ms, the diffusion for the triangular void was still limited by the reduced contact area near its top peak, thus restricting the efficient transmission of moisture to the surrounding elements. By contrast, the flat top edge in the inverted triangular increased the contact area of the hydrophilic void and, therefore, transmitted the moisture to the below elements more effectively. The upper broader contact area of the IT model led to a more uniform and rapid diffusion of moisture, compared to the case of the narrower apex for the standard triangular void. However, after 20 ms, as the moisture concentration on the side of the triangular voids increased; the IT model had a higher diffusivity than the T model. Furthermore, by this time, the model with the circular void of 0.15 mm achieved a moisture concentration of 0.5%, which was significantly faster than the pure-matrix model. This saturation time was approximately 1/2 compared to that of the PM model. Hence, the large hydrophilic void significantly accelerated the diffusion process.

The mass flow rate contour (Figure 6) provides additional information for understanding the diffusion process and specific features of its realisation for voids of different types, shapes and dimensions. The grey zones in the contour plots are areas with the flow rate exceeding the maximum value defined in the figure legend. Notably, these extreme values were observed at the top of the T model for the hydrophilic (Type II) void. This phenomenon is due to the small mesh size in the simulation of the areas around the apexes, which resulted in artificially high mass flow rates. Compared to the IT model, the void of the T model primarily absorbs moisture from the peak area, with the mass flow rate in its wing area being significantly lower than that in the wings of the IT model. Furthermore, the peak of the IT model also diffused moisture to the horizontally adjacent elements. In all Type II models, the central region of the part adjacent to the moisture boundary had a higher mass flow rate compared to its side elements. This is caused by the high

diffusivity of such voids, which attracted moisture and then transferred it to areas with lower concentrations. As a result, higher fluid transport occurred in the central parts of the domain. In contrast to the Type I void models, the low mass flow rate in the bottom central area was not present for Type II models. Moisture from the void penetrated the bottom interface and, hence, had a different moisture path.

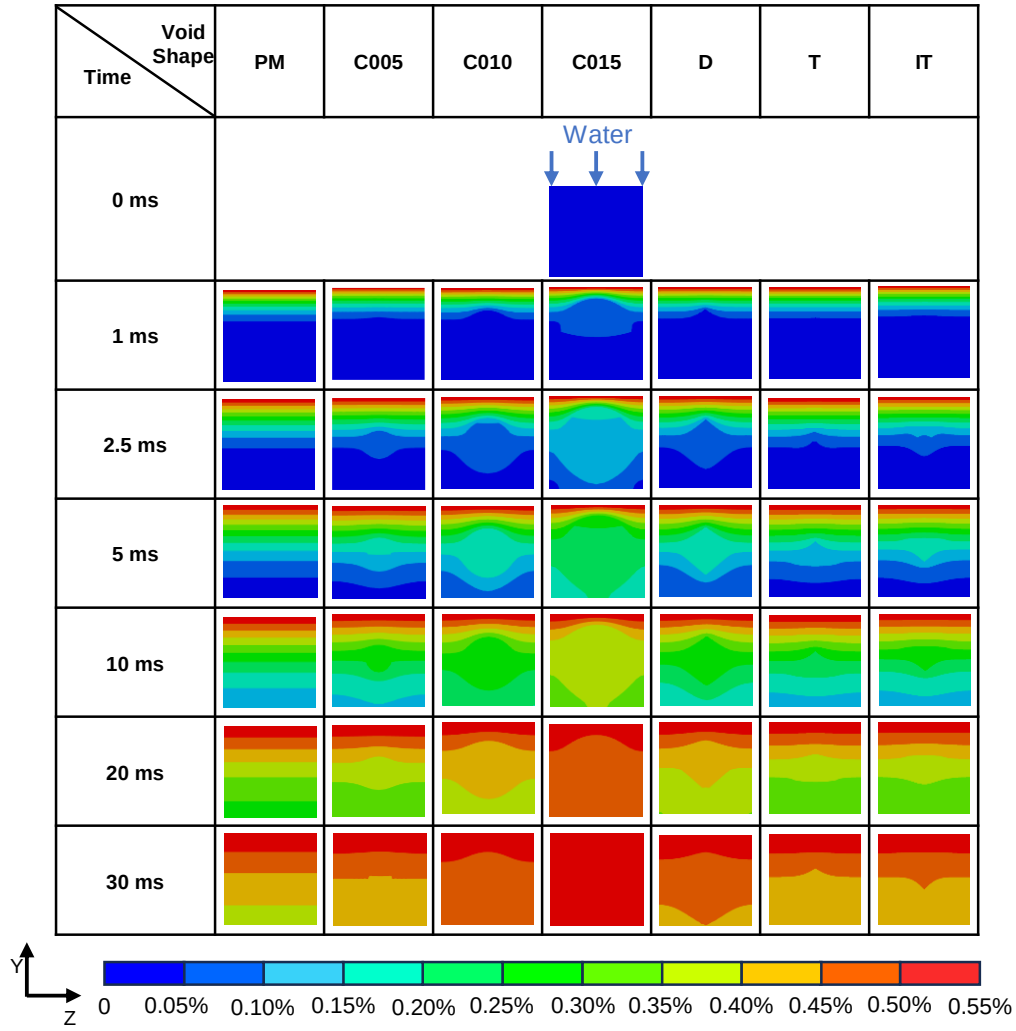

Figure 7. Spatial evolution of water uptake process for different voids of Type II.

4. Conclusions

In this study, multiple finite-element models of a polymer matrix with voids were developed to investigate the effect of voids in printing beads, inherent in MEAM products, in the diffusion process in PETG. The results of the simulations indicate that the voids created during the manufacturing of 3D-printed composites significantly affected the water diffusion process in them.

It was established that the hydrophobic voids significantly retarded the diffusion of moisture in the composite model. The time required to reach a 90% saturation state can be up to a 1/3 longer, depending on the size and shape of the void. This became more pronounced for the higher porosity and voids occupying considerable parts of the cross-section available for diffusion. In general, hydrophobic voids limit the propagation of moisture in the polymer matrix.

In contrast, hydrophilic voids considerably accelerated the diffusion process. The time to reach a 90% saturation state can be reduced by up to 50% compared to the pure-matrix model. The high diffusivity of these voids enabled them to act as channels, transferring

moisture to adjacent elements. The overall diffusivity of the composite model with hydrophilic voids was predominantly influenced by the void volume fraction. Larger voids with high diffusivity enhanced moisture distribution and reduced the time required to reach saturation compared to the pure matrix.

This study investigates the impact of different void characteristics on the moisture diffusion process in the PETG matrix. It can be concluded that in the design of 3D-printed components for marine environments, voids with their main geometrical features are an important feature to consider.

Author Contributions: Conceptualisation, B.L., K.P.B. and V.V.S.; methodology, B.L.; software, B.L.; formal analysis, B.L.; writing—original draft preparation, B.L.; writing—review and editing, K.P.B. and V.V.S.; visualisation, B.L.; supervision, K.P.B. and V.V.S. All authors have read and agreed to the published version of the manuscript.

Funding: This research received no external funding.

Data Availability Statement: The data supporting the conclusions of this article will be made available by the authors on request.

Conflicts of Interest: The authors declare no conflicts of interest.

References

1. Ziółkowski, M.; Dyl, T. Possible applications of additive manufacturing technologies in shipbuilding: A review. *Machines* **2020**, *8*, 84. [CrossRef]
2. Rawal, S.; Karabudak, N. Additive manufacturing of Ti-6Al-4V alloy components for spacecraft applications. In Proceedings of the RAST 2013—Proceedings of 6th International Conference on Recent Advances in Space Technologies, Istanbul, Turkey, 12–14 June 2013; pp. 5–11.
3. Zhang, K.; Wang, Q. Mechanical characterization of hybrid lattice-to-steel joint with pyramidal CFRP truss for marine application. *Compos. Struct.* **2017**, *160*, 1198–1204. [CrossRef]
4. Shuai, C.; Pan, H. Accelerated degradation of HAP/PLLA bone scaffold by PGA blending facilitates bioactivity and osteoconductivity. *Bioact. Mater.* **2021**, *6*, 490–502. [CrossRef] [PubMed]
5. Dydek, K.; Boczkowska, A. Thermal, rheological and mechanical properties of PETG/RPETG blends. *J. Polym. Env.* **2019**, *27*, 2600–2606.
6. Li, W.; Zhao, X.; Liu, Y.; Ouyang, Y.; Li, W.; Chen, D.; Ye, D. Hygrothermal aging behavior and flexural property of carbon fiber-reinforced polyethylene terephthalate glycol composites. *Text. Res. J.* **2023**, *93*, 1005–1018. [CrossRef]
7. Ramírez-Revilla, S.; Márquez, G. Evaluation and comparison of the degradability and compressive and tensile properties of 3D printing polymeric materials: PLA, PETG, PC, and ASA. *MRS Commun.* **2023**, *13*, 55–62. [CrossRef]
8. Dhakal, H.N.; Bennett, N. Development of flax/carbon fibre hybrid composites for enhanced properties. *Carbohydr. Polym.* **2013**, *96*, 1–8. [CrossRef] [PubMed]
9. Pérez, M.; Carou, D. Surface quality enhancement of Fused Deposition Modeling (FDM) printed samples based on the selection of critical printing parameters. *Materials* **2018**, *11*, 1382. [CrossRef] [PubMed]
10. Hussnain, S.M.; Hussain, M.Z. Degradation and mechanical performance of fibre-reinforced polymer composites under marine environments: A review of recent advancements. *Polym. Degrad. Stab.* **2023**, *215*, 110452. [CrossRef]
11. Bellini, A.; Güçeri, S. Mechanical characterization of parts fabricated using fused deposition modeling. *Rapid Prototyp. J.* **2003**, *9*, 252–264. [CrossRef]
12. Tao, Y.; Kong, F.; Li, Z.; Zhang, J.; Zhao, X.; Yin, Q.; Xing, D.; Li, P. A review on voids of 3D printed parts by fused filament fabrication. *J. Mater. Res. Technol.* **2021**, *15*, 4860–4879. [CrossRef]
13. Kumar, M.; Omarbekova, A. 3D printed polycarbonate reinforced acrylonitrile–butadiene–styrene composites: Composition effects on mechanical properties, micro-structure and void formation study. *J. Mech. Sci. Technol.* **2019**, *33*, 5219–5226. [CrossRef]
14. Tao, Y. A case study: Mechanical modeling optimization of cellular structure fabricated using wood flour-filled polylactic acid composites with fused deposition modeling. *Compos. Struct.* **2019**, *216*, 360–365. [CrossRef]
15. Goh, G.D.; Dikshit, V.; Nagalingam, A.P.; Goh, G.L.; Agarwala, S.; Sing, S.L.; Wei, J.; Yeong, W.Y. Characterization of mechanical properties and fracture mode of additively manufactured carbon fiber and glass fiber reinforced thermoplastics. *Mater. Des.* **2018**, *137*, 79–89. [CrossRef]
16. Fichera, M.; Carlsson, L.A. Moisture transport in unidirectional carbon/vinylester panels with imperfect fiber/matrix interface. *J. Compos. Mater.* **2016**, *50*, 751–760. [CrossRef]
17. Carlsson, L.A.; Du, E. Water uptake in polymer composites with voids. *Durab. Compos. A Mar. Environ.* **2018**, *245*, 33–57.
18. Tekinalp, H.L.; Kunc, V.; Velez-Garcia, G.M.; Duty, C.E.; Love, L.J.; Naskar, A.K.; Blue, C.A.; Ozcan, S. Highly oriented carbon fiber–polymer composites via additive manufacturing. *Compos. Sci. Technol.* **2014**, *105*, 144–150. [CrossRef]

19. Abdelmola, F.; Carlsson, L.A. Water uptake in epoxy matrix with voids: Experiments and modeling. *J. Compos. Mater.* **2019**, *53*, 1049–1065. [CrossRef]
20. Wang, M. Multiscale water diffusivity prediction of plain woven composites considering void defects. *Sci. Eng. Compos. Mater.* **2024**, *31*, 20220236. [CrossRef]
21. Bourennane, H.; Gueribiz, D.; Fréour, S.; Jacquemin, F. Modeling the effect of damage on diffusive behavior in a polymeric matrix composite material. *J. Reinf. Plast. Compos.* **2019**, *38*, 717–733. [CrossRef]
22. Little, J.E.; Yuan, X.; Jones, M.I. Characterisation of voids in fibre reinforced composite materials. *NDT E Int.* **2012**, *46*, 122–127. [CrossRef]
23. Chen, Y.; Klingler, A.; Fu, K.; Ye, L. 3D printing and modelling of continuous carbon fibre reinforced composite grids with enhanced shear modulus. *Eng. Struct.* **2023**, *286*, 116165. [CrossRef]
24. Liu, Z.; Zhang, J. Effect mechanism and simulation of voids on hygrothermal performances of composites. *Polymers* **2022**, *14*, 901. [CrossRef] [PubMed]
25. Cussler, E.L. *Diffusion: Mass Transfer in Fluid Systems*, 2nd ed.; Cambridge University Press: Cambridge, UK, 1997; p. 600.